



RESEARCH

A multimodal study of brain regions in pediatric epilepsy: anatomical, radiological, and machine learning approaches

Pediyatrik epilepside beyin bölgelerinin çok yönlü bir çalışması: anatomik, radyolojik ve makine öğrenimi yaklaşımları

Kübra Kulaz¹, Mahmut Öksüzler², Faruk İncecik¹, Berkay Dik¹, Ömer Kaya¹, Önder Çoban³, Mahmut Tunç⁴, Neslihan Boyan¹, Pınar Göker¹, Sema Polat¹

¹Çukurova University, Adana, Türkiye

²Bozyaka Education and Research Hospital, İzmir, Türkiye

³Atatürk University, Erzurum, Türkiye

⁴Başkent University, Adana, Türkiye

Abstract

Purpose: This study aims to investigate the anatomical and radiological differences in brain regions between pediatric epilepsy patients and age-matched healthy controls without neurological sequelae, by machine learning techniques.

Materials and Methods: This study comprised 78 neurologically healthy children (mean age: 7.25 ± 4.25 years) and 101 pediatric patients diagnosed with epilepsy (mean age: 6.91 ± 4.34 years), all of whom underwent comprehensive anatomical and radiological evaluation. Magnetic Resonance Imaging was used to measure the volumes of the amygdaloid complex, hippocampus, insula, thalamus, caudate nucleus, the largest area of the brain, and the corpus callosum.

Results: These volumetric measurements were generally higher in healthy children compared to those with epilepsy. Notably, the differences in the volumes of the amygdaloid complex, insula, and corpus callosum were statistically significant between the epilepsy and control groups. Significant reductions in the volumes of key brain regions including the hippocampus, corpus callosum, thalamus, and overall cortical surface in children with epilepsy compared to healthy controls.

Conclusion: This study may contribute Machine learning methods combined with carefully selected features have demonstrated exceptional accuracy and reliability in the automatic detection of epilepsy, underscoring their significant potential to enhance clinical diagnostics and facilitate personalized treatment strategies.

Keywords: Machine learning, neuroanatomical changes, pediatric epilepsy

Öz

Amaç: Bu çalışma, makine öğrenimi tekniklerini kullanarak pediyatrik epilepsi hastaları ile nörolojik sekeli olmayan yaşları uyumlu sağlıklı kontrol grubu arasındaki beyin bölgelerindeki anatomik ve radyolojik olarak varolabilecek farklılıkları araştırmayı amaçlar.

Gereç ve Yöntem: Bu çalışmada herhangi bir nörolojik sekeli bulunmayan 78 sağlıklı çocuk (ortalama yaş: $7,25 \pm 4,25$ yıl) ve 101 epilepsi tanısı almış çocuk hasta (ortalama yaş: $6,91 \pm 4,34$ yıl) kapsamlı anatomik ve radyolojik değerlendirmeler yapılmıştır. Manyetik Rezonans Görüntüleme, corpus amygdaloideum, hippocampus, insula, thalamus, nucleus caudatus, beyin en geniş alanı ve corpus callosum hacimlerini ölçmek için kullanıldı.

Bulgular: Bu hacimsel ölçümler sağlıklı çocuklarda epilepsi teşhisi konmuş olanlara kıyasla daha yüksekti. Özellikle, corpus amygdaloideum, insula ve corpus callosum hacimlerindeki farklılıklar epilepsi ve kontrol grupları arasında istatistiksel olarak anlamlıydı. Sağlıklı kontrollere kıyasla epilepsili çocuklarda hippocampus, corpus callosum, thalamus ve genel kortikal yüzey dahil olmak üzere önemli beyin bölgelerinin hacimlerinde önemli azalmalar olduğunu ortaya koymaktadır.

Sonuç: Özenle seçilmiş özelliklerle birleştirilen makine öğrenimi yöntemleri, epilepsinin otomatik olarak tespit edilmesinde olağanüstü doğruluk ve güvenilirlik göstererek, klinik teşhisi geliştirme ve kişiselleştirilmiş tedavi stratejilerini kolaylaştırma konusundaki önemli potansiyellerin altını çizmiştir.

Anahtar kelimeler: Makine öğrenmesi, nöroanatomik değişiklikler, pediyatrik epilepsi

Address for Correspondence: Sema Polat, Cukurova University Faculty of Medicine, Department of Anatomy, Adana, Türkiye E-mail: sezaoz@hotmail.com

Received: 13.06.2025 Accepted: 12.12.2025

INTRODUCTION

Epilepsy is a chronic neurological disorder marked by an enduring predisposition of the brain to generate recurrent epileptic seizures, accompanied by a complex spectrum of neurobiological, cognitive, psychosocial, and societal consequences. These outcomes are largely driven by both morphological and metabolic alterations within the brain. Seizures, the hallmark clinical manifestation of epilepsy, may occur at any age and result from abnormal, excessive neuronal discharges in the cerebral cortex and are often associated with significant motor and cognitive impairments, and decrease in quality of life¹⁻⁴. According to the World Health Organization (WHO), epilepsy affects over 70 million individuals globally, including approximately 10.5 million children. Compelling evidence underscores a strong genetic predisposition underlying epilepsy, with genetic factors accounting for an estimated 70-80% of cases. Furthermore, the burden of epilepsy disproportionately impacts low- and middle-income countries, where its prevalence is notably higher¹.

Childhood is an important and critical period of brain development, particularly the first year of life when important motor and cognitive milestones are achieved and brain volume almost doubles⁵⁻⁷. As brain development continues, synaptic connections initially form rapidly, with an increase in grey matter volume and white matter volume increase that continues to increase until approximately 10 years of age^{6,8,9}. As this is an important time for brain development and maturation, microstructural changes in these regions may contribute to the developmental difficulties experienced by children with epilepsy. This may play a critical role in the development of worse neuro-psychosocial outcomes in adulthood⁶. Although epilepsy is a prevalent and impactful neurological disorder in pediatric populations, its effects on the developing brain remain relatively underexplored compared to adults. Emerging evidence, however, indicates that epilepsy can significantly disrupt neurocognitive development and impair cognitive performance during critical periods of childhood^{2,5,6,10}.

Magnetic Resonance Imaging (MRI) is a safe, non-invasive, and highly effective technique for detecting structural abnormalities in the central nervous system associated with epilepsy. It offers high-resolution visualization of key brain regions, such as the

hippocampus and corpus callosum (CC), facilitating the identification of seizure foci, guiding treatment strategies, and optimizing surgical outcomes particularly in pediatric populations^{3,5,11-15}. In our study, MRI was used to better illustrate the link between epilepsy and structural brain abnormalities.

This study demonstrates significant volume reductions in key brain regions, including the hippocampus, corpus callosum, thalamus, and cortical surface, in children with epilepsy. These findings suggest that epilepsy should be considered not only a functional but also a structural brain disorder. Furthermore, the artificial intelligence-based analysis methods used in the study point to the potential of advanced technologies to enhance diagnostic processes in evaluating brain morphology in epilepsy and offer an innovative approach to clinical decision-making processes. Thus, the study both expands the knowledge base on the neurobiological mechanisms of epilepsy and contributes to the literature by supporting the effectiveness of new analytical tools that can be used in clinical practice.

In this study, our hypothesis is that the hippocampus, thalamus, and corpus callosum in children with epilepsy are significantly lower than in healthy peers, and that artificial intelligence-based morphometric analysis methods detect epilepsy-related structural brain changes with higher accuracy than traditional imaging assessments.

MATERIALS AND METHODS

Sample

The study included 78 healthy children (34 girls, 44 boys) aged between 0 and 15 years with no known health issues, and 101 children (36 girls, 65 boys) in the same age range diagnosed with epilepsy. The sample calculation in the study was made according to individuals who met the inclusion criteria. This study was a retrospective observational study conducted in the Department of Radiology at Bozyaka Education and Research Hospital, University of Health Sciences, İzmir, and Çukurova University, Faculty of Medicine, Department of Pediatrics Neurology, Adana. Magnetic Resonance Image analyses were performed by an experienced radiologist (observer 1, radiologist MÖ). The other two experienced radiologists (Observer 2, radiologist ÖK and observer 3, radiologist BT) contributed to

the development of the study protocol during the planning phase and independently reviewed a limited number of randomly selected cases to assess the reliability of the measurements (ICC = 0.720). At the start of the study, 123 children with epilepsy were included. Of these, 16 cases had cerebral palsy accompanying epilepsy. The MRI images of 6 of them were not clear enough to calculate the field measurements. Among the healthy children included in the study, 85 children were found to be suitable at the outset. However, the MRI images of 4 healthy children did not contain the measurement parameters included in the study. The MRI images of 3 children were also unclear.

Also, epilepsy diagnosis was made by an experienced a child neurologist (pediatric neurologists FI). Additionally, the data were obtained from official hospital records, and all file security procedures were carried out in accordance with the protocols established by the relevant institution. Ethical approval for the study was obtained from the Non-Invasive Clinical Research Ethics Committee of Çukurova University, with registration number 136;43 dated 2023 and an additional decision numbered 146;7 dated 2024. Among the 101 children with epilepsy, 25 were diagnosed with abnormal EEG findings of unknown etiology, 22 with complex focal epilepsy, 12 with simple focal epilepsy, and 42 with generalized tonic-clonic epilepsy

Inclusion criteria for children with epilepsy were to have been diagnosed with epilepsy by a pediatric neurologist, to be between the ages of 0-15, not having any additional neurological, neuromuscular, or neurodegenerative diseases and secondary diseases affecting the musculoskeletal system, no comorbidity accompanying epilepsy, not to have undergone any surgery related to the brain and spinal cord, and

having no history of tumor, trauma, infection, etc. in related structures.

Inclusion criteria for children in the control group were to be between the ages of 0-15 years, not having an additional neurological, neuromuscular or secondary disease affecting the musculoskeletal system, not having a history suggestive of epilepsy, not to have undergone any surgery related to the brain and spinal cord and having no history of tumour, trauma, infection etc. in the related structures.

Study design

MRI images were acquired using a 1.5T Siemens Magnetom Aera scanner (Siemens Healthcare, Erlangen, Germany) with a 20-channel head coil. Images were acquired in the axial and sagittal planes using a T1-weighted MP-RAGE sequence using the following parameters: TR = 2400 ms, TE = 3.54 ms, FOV = 240 mm, slice thickness = 1.2 mm, and voxel size = $1.3 \times 1.3 \times 1.2$ mm. Area measurements of anatomical structures were performed manually on the most appropriate slice selected by the radiologist using the PACS program available in the hospital system. Also, area measurements were performed for specific brain regions, including the amygdaloid complex, hippocampus, insula, thalamus, caudate nucleus, the largest cross-sectional area of the brain, and the corpus callosum. The calculated areas were recorded in square centimeters (cm²) for both the left and right hemispheres (Figure 1).

Importantly, machine learning methods combined with carefully selected features have been used to automatically detect epilepsy, improving clinical diagnosis and facilitating personalised treatment strategies.

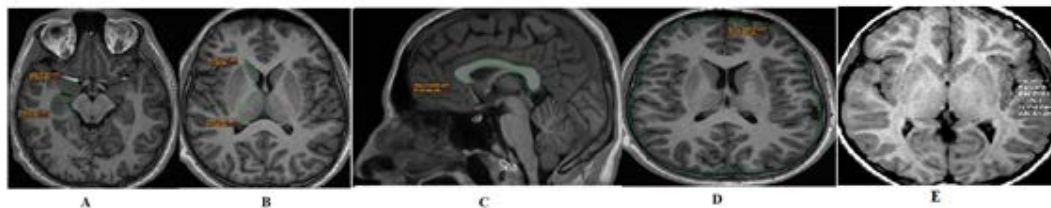


Figure 1. The different brain region's Magnetic Resonance Imaging. A. Amygdaloid complex and hippocampus head area measurement in patients with epilepsy in the axial plane, B. Measurement of caudate nucleus caput and thalamus area in patients with epilepsy in the axial plane, C. Corpus callosum area measurement in patients with epilepsy in the sagittal plane, D. Measurement of the largest area of the brain in patients with epilepsy in the axial plane, E. Measurement of the insula in the axial plane..

ML-based prediction of epilepsy

Dataset

In this study, a dataset that includes 15 attributes of 179 children. Our target feature consists of two values showing if the respective instance has epilepsy or not. On the other hand, the rest of the features include gender, age, age range, and some other features derived based on specific measurements. Table 1 presents the distribution of instances for both gender and target features. These methods to perform ML-based epilepsy prediction include well-known techniques used in supervised classification tasks. The first step is preprocessing. It is two simple sub-steps which are briefly described as follows:

$$AF(f_{\text{all}}) = \frac{\overbrace{\sum_{i=1}^k \frac{n_i(\bar{X}_i - \bar{X})^2}{k-1}}^{\sigma_{\text{BCV}}^2}}{\underbrace{\sum_{i=1}^k \sum_{j=1}^{n_i} \frac{(X_{ji} - \bar{X}_i)^2}{N-k}}_{\sigma_{\text{WCV}}^2}}$$

Figure 2. Formal definition of the ANOVA-based feature selector.

In scaling, which is used to transform feature values, each value is normalized to fall within a predefined range, typically between 0 and 1¹⁶. The one-hot encoding step converts categorical features into multiple binary variables. Each category is mapped to a separate variable with a value of either 0 (indicating absence) or 1 (indicating presence)¹⁷. Additionally, feature selection is one of the two main approaches to dimensionality reduction in machine learning, the other being feature extraction. In this study, the filter-based feature selection which first relies on ranking features based on any goodness function that may be any metric or measurement is employed¹⁸.

It secondly, selects the top n best features considering their ranking scores. The ANOVA function is chosen for this study both because it is

one of the well-known filter-based feature selectors and because it is formally described as depicted in Figure 2^{19,20}. Moreover, Classification is the most important step to building an ML pipeline since the core property of such a supervised pipeline is the classification phase that is achieved by using classifiers. In this study, ML classifiers are described briefly as follows (Table 1)^{16,20-28}:

The performance of any ML pipeline is measured by using four values namely True Positive (TP), False Positive (FP), False Negative (FN), and True Negative (TN) which are derived from the confusion matrix. In this study, we use the f1 score which is one of the well-known performance metrics and robust across the imbalanced nature of any dataset at hand. It is calculated by taking the harmonic mean of Precision (P) and Recall (R) and formally described as follows^{16,20}:

$$F1 \text{ Score} = 2 * \frac{P * R}{P + R}$$

In the above equation, $P = TP / (TP + FP)$ and $R = TP / (TP + FN)$. Furthermore, in the field of machine learning, an evaluation method favoured as cross-validation is often employed, which is based on the division of the available dataset into training and test subsets²⁹. In this paper, we evaluate all classifiers using stratified five-fold cross-validation and report the average f1 score across the five folds, as prescribed by the method to ensure that the evaluation is unbiased. Stratification means that samples are selected in the same proportion to appear in the test set as they appear in the training set²⁰.

Statistical analysis

Statistical Package for the Social Sciences (SPSS) version 21.0 software was used. In all statistical analyses, a p-value under 0.05 was considered to be statistically significant. The Kolmogorov-Smirnov test was used to determine whether the study was parametric or non-parametric. Based on the analysis of the measurements, the following statistical methods were applied. The p-values for brain area measurements in subjects diagnosed with epilepsy and in healthy subjects were analyzed using ANOVA. A Post hoc test was conducted to assess age-related changes.

Table 1. ML classifiers' names and definitions

Classification	Definition
Multi-Layer Perceptron (MLP)	This classifier consists of more than one perceptron. It is actually type of a feed-forward artificial neural network. It is often structured to include input, single hidden, and output layers. The hidden layer is responsible for detecting nonlinear decision boundaries by learning the correlation between input/output layers ^{16,21} .
Decision Tree (DT)	This classifier creates an abstract tree consisting of branches and nodes such that the entire path from the root node to any of the leaf nodes represents one classification rule ^{20,22,23} .
Naïve Bayes (NB)	It is a probabilistic classifier relying on Bayes' theorem and has the advantage. A small amount of data is enough to learn classification parameters ^{20,22,23} .
Multinomial NB (MNB)	It uses the Bayesian learning perspective and unlike the NB classifier, it assumes that feature distributions in samples are generated by a specific parametric model ²⁴ .
<i>k</i> -Nearest Neighbor (KNN)	This is known as a lazy learner and relies on the simple principle that instances having similar properties should have proximity. The final decision is given by identifying the most frequent label (or target) among the labels of any test instance's <i>k</i> neighbors ^{20,23} .
Support Vector Machine (SVM)	This is a non-probabilistic classifier that relies on margin calculation. It is used to analyze vectorized data and find a hyperplane that separates two inputs from each other ^{20,22} .
Gradient Boosting Classifier (GBC)	This is another type of ensemble learner and it creates new base learners that are maximally correlated with the negative gradient of the loss function associated with the entire ensemble ²⁴⁻²⁶ .
Random Forest (RF)	This classifier takes place in the family of ensemble learning algorithms and can be used for both classification and regression. Its final decision for any test instance is given by combining the outputs of multiple DTs ^{16,20} .
Logistic Regression (LR)	This method can be used for both classification and regression tasks. It tries to learn the relationship between any number of features and target value. Its final decision for a test instance is given by using parameter values that are learned in the training phase with the condition that they should provide maximum likelihood ^{20,27} .
AdaBoost (AB)	This is an ensemble classifier that uses the boosting technique to combine multiple weak classifiers into a single strong classifier ^{16,23,28} .

RESULTS

The mean age of boys and girls with epilepsy was 6.91 ± 4.34 years (2 months, min.; 15 years, max.), while the mean age of healthy boys, and girls aged 0-13 years was 7.25 ± 4.25 years (3 months, min.; 13 years, max.) ($p=0.600$). Additionally, in the epilepsy and healthy control groups, the amygdaloid complex, hippocampus head, insula, caudate nucleus head, thalamus, corpus callosum, and the largest area of the brain were measured. All measurements were found to be higher in the healthy control group than in the epilepsy group, but only three measurements including the amygdaloid complex, insula, and corpus callosum were statistically significant ($p < 0.05$) (Table 2). Moreover, brain area measurements in subjects diagnosed with epilepsy and healthy controls according to gender were given in Table 3. From these findings, only 4 parameters including the hippocampus head, thalamus, CC, and the largest brain area showed a statistically significant difference between genders in subjects diagnosed with Epilepsy.

Additionally, the age-related changes of the brain area measurements in both subjects diagnosed with Epilepsy, and healthy controls were shown in Tables 4 and 5. All parameters were significantly different in both subjects with Epilepsy and healthy subjects in terms of age-related changes.

To obtain our results, firstly, Python core libraries as well as some other ones including Pandas, Scikit-learn, and NumPy is set up ^{20,30,31}. Using these methods, different cases (or scenarios) are constituted to create a basic ML pipeline for the automatic detection of epilepsy (Table 6). As seen in Table 6, our cases is created by considering the features. Afterward, prediction results were obtained using stratified five-fold cross-validation on the six datasets generated in the cases inf Table 6. The obtained results are presented in Table 7 where the results with bold typeset represent the best f1-score for the case at hand.

As seen in Table 7, classifiers including DT, GBC, RF, and AB are often superior to other classifiers

almost in all cases. On the other hand, the best classifier is GBC in all cases and achieves best f1 scores of 0.710, 0.698, 0.709, 0.734, and 7.24 for cases A, B, C, D, and E respectively. These results show that the best option among the first six cases is case D which involves only one-hot-encoding on gender and age features. As seen in Figure 3, f1 scores of classifiers have a decreasing trend when the number of selected features is increasing. The most robust classifier seems to be GBC across the data nature, but the best f1 score of 0.771 is obtained by the DT classifier by using the most informative four features.

An overall evaluation of these results together with that of the ones obtained in the previous six cases shows that feature selection improves classification f1 score. On the other hand, as seen in Table 8, the most informative four features selected in the case of F across five-folds are often comprised of the left amygdala, right amygdala, left insular cortex, and right insular cortex. Hence, it is clear that these features should be evaluated to have more weight when detecting if any child is epilepsy by using any automatic (e.g., ML) or hand-crafted way.

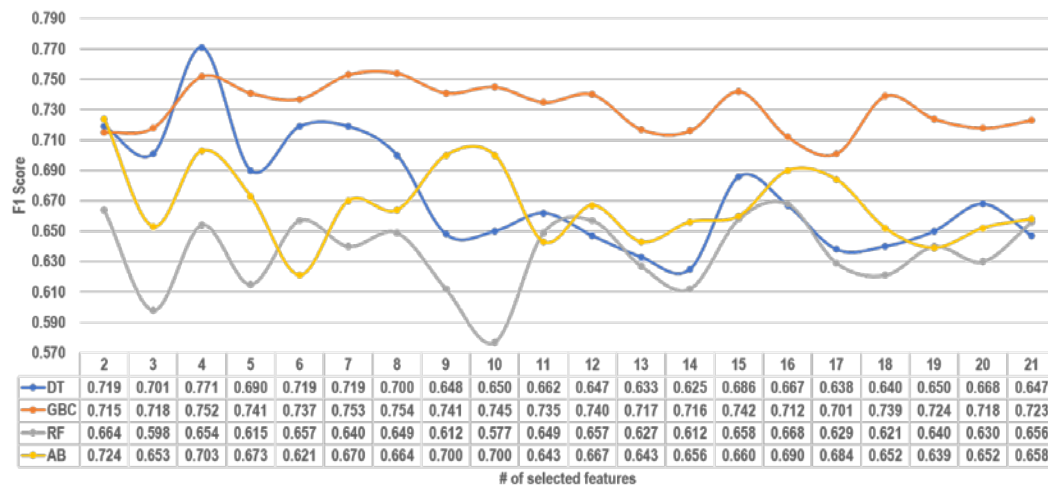


Figure 3. The F1 scores of four superior classifiers across different numbers of selected features in case F.

Table 2. Brain area measurements in subjects diagnosed with epilepsy and in healthy controls

Measurements (cm ²)	Subjects diagnosed with epilepsy (n=101)	Healthy controls (n=78)	P value
	Mean±SD	Mean±SD	
Amygdaloid complex (Right)	1.089±0.27	1.20±0.19	0.002
Amygdaloid complex (Left)	1.094±0.25	1.17±0.18	0.020
Hippocampus head (Right)	1.48±0.61	1.53±0.60	0.549
Hippocampus head (Left)	1.44±0.51	1.54±0.52	0.212
Insula (Right)	2.94±.68	3.18±0.52	0.009
Insula (Left)	2.93±0.67	3.19±0.51	0.004
Caudate nucleus head (Right)	1.24±0.27	1.28±0.23	0.292
Caudate nucleus head (Left)	1.26±0.26	1.30±0.23	0.341
Thalamus (Right)	4.065±0.71	4.13±0.55	0.471
Thalamus (Left)	4.061±0.70	4.15±0.52	0.372
The largest brain area	150.18±20.23	155.31±16.53	0.071
Corpus callosum area	4.49±1.14	4.87±1.15	0.032

Table 3. Brain area measurements in subjects diagnosed with epilepsy and healthy controls according to gender

Measurements (cm ²)	Subjects diagnosed with Epilepsy (n=101)		Healthy controls (n=78)	
	Girls (n=36)	Boys (n=65)	Girls (n=34)	Boys (n=44)
	Mean±SD	Mean±SD	Mean±SD	Mean±SD
Amygdaloid complex (Right)	1.04±0.30	1.12±0.25	1.21±0.19	1.19±0.19
<i>P value</i>	0.191		0.594	
Amygdaloid complex (Left)	1.03±0.26	1.13±0.23	1.19±0.18	1.16±0.17
<i>P value</i>	0.560		0.555	
Hippocampus head (Right)	1.30±0.35	1.54±0.70	1.52±0.41	1.57±0.69
<i>P value</i>	0.030		0.862	
Hippocampus head (Left)	1.28±0.30	1.52±0.58	1.52±0.36	1.54±0.62
<i>P value</i>	0.028		0.860	
Insula (Right)	2.92±0.63	2.94±0.70	3.30±0.52	3.09±0.50
<i>P value</i>	0.881		0.066	
Insula (Left)	2.91±0.64	2.93±0.69	3.32±0.49	3.10±0.50
<i>P value</i>	0.890		0.050	
Caudate nucleus head (Right)	1.18±0.27	1.27±0.27	1.25±0.23	1.29±0.23
<i>P value</i>	0.104		0.429	
Caudate nucleus head (Left)	1.20±0.25	1.30±0.26	1.28±0.24	1.32±0.22
<i>P value</i>	0.053		0.448	
Thalamus (Right)	3.81±0.57	4.14±0.53	4.13±0.54	4.20±0.74
<i>P value</i>	0.009		0.617	
Thalamus (Left)	3.76±0.53	4.15±0.53	4.14±0.50	4.22±0.73
<i>P value</i>	0.001		0.601	
The largest brain area	141.89±19.12	154.58±19.54	150.76±16.31	158.82±16.00
<i>P value</i>	0.020		0.032	
Corpus callosum	4.16±0.68	4.67±1.29	5.06±1.26	4.72±1.04
<i>P value</i>	0.030		0.197	

Table 4. The age-related changes of the brain area measurements in subjects diagnosed with Epilepsy

Measurements (cm ²)	Subjects diagnosed with Epilepsy (n=101)						
	0-1 years (n=13)	2-3 years (n=16)	4-6 years (n=20)	7 years (n=10)	8-9 years (n=9)	10-11 years (n=12)	12 years and over (n=21)
	Mean±SD	Mean±SD	Mean±SD	Mean±SD	Mean±SD	Mean±SD	Mean±SD
Amygdaloid complex (Right)	0.72±0.18	1.03±0.19	1.00±0.20	1.14±0.17	1.20±0.23	1.29±0.12	1.26±0.26
<i>P value</i>	<0.001						
Amygdaloid complex (Left)	0.72±0.17	1.03±0.16	1.02±0.19	1.17±0.15	1.20±0.18	1.25±0.14	1.27±0.21
<i>P value</i>	<0.001						
Hippocampus head (Right)	0.96±0.23	1.66±0.93	1.47±0.78	1.45±0.20	1.43±0.24	1.46±0.25	1.71±0.53
<i>P value</i>	0.025						
Hippocampus head (Left)	0.98±0.22	1.61±0.79	1.44±0.68	1.43±0.22	1.42±0.24	1.45±0.22	1.59±0.32
<i>P value</i>	0.002						

Insula (Right)	1.84±0.56	3.14±0.71	2.85±0.39	3.37±0.38	3.10±0.69	2.96±0.54	3.25±0.36
<i>P value</i>	<0.001						
Insula (Left)	1.86±0.56	3.02±0.62	2.91±0.44	3.34±0.52	2.98±0.67	3.04±0.55	3.24±0.40
<i>P value</i>	<0.001						
Caudate nucleus head (Right)	0.81±0.20	1.17±0.21	1.23±0.20	1.37±0.19	1.28±0.18	1.42±0.15	1.37±0.23
<i>P value</i>	<0.001						
Caudate nucleus head (Left)	0.84±0.19	1.23±0.21	1.26±0.21	1.36±0.17	1.29±0.18	1.43±0.12	1.41±0.20
<i>P value</i>	<0.001						
Thalamus (Right)	3.36±0.61	4.00±0.56	3.79±0.59	4.23±0.46	4.19±0.75	4.49±0.56	4.43±0.75
<i>P value</i>	<0.001						
Thalamus (Left)	3.29±0.53	4.01±0.61	3.81±0.53	4.23±0.44	4.21±0.73	4.48±0.50	4.43±0.75
<i>P value</i>	<0.001						
The largest brain area	117.08±16.72	143.75±12.27	147.40±17.38	161.90±10.19	158.56±13.97	160.17±10.43	163.33±14.12
<i>P value</i>	<0.001						
Corpus callosum area	3.21±0.64	3.69±0.58	4.35±0.48	4.38±1.12	4.63±0.73	5.29±0.88	5.58±1.16
<i>P value</i>	<0.001						

Table 5. The age-related changes of the brain area measurements in healthy controls

Measurements (cm ²)	Healthy controls (n=78)						
	0-1 years (n=11)	2-3 years (n=10)	4-6 years (n=14)	7 years (n=5)	8-9 years (n=7)	10-11 years (n=14)	12 years and over (n=17)
	Mean±SD	Mean±SD	Mean±SD	Mean±SD	Mean±SD	Mean±SD	Mean±SD
Amygdaloid complex (Right)	0.83±0.09	1.13±0.07	1.21±0.12	1.37±0.04	1.30±0.09	1.33±0.12	1.28±0.10
<i>P value</i>	<0.001						
Amygdaloid complex (Left)	0.86±0.08	1.18±0.08	1.22±0.13	1.09±0.17	1.20±0.18	1.24±0.13	1.29±0.11
<i>P value</i>	<0.001						
Hippocampus head (Right)	1.02±0.09	1.90±1.05	1.43±0.07	1.47±0.26	1.89±1.18	1.46±0.25	1.66±0.31
<i>P value</i>	0.008						
Hippocampus head (Left)	1.11±0.12	1.85±0.93	1.48±0.10	1.45±0.32	1.81±1.04	1.44±0.23	1.66±0.30
<i>P value</i>	0.017						
Insula (Right)	2.65±0.36	3.29±0.32	3.45±0.41	3.34±0.43	2.87±0.46	2.96±0.51	3.50±0.45
<i>P value</i>	<0.001						
Insula (Left)	2.74±0.33	3.31±0.29	3.45±0.37	3.29±0.67	2.73±0.38	3.03±0.52	3.51±0.43
<i>P value</i>	<0.001						
Caudate nucleus head (Right)	0.96±0.17	1.14±0.11	1.22±0.15	1.27±0.22	1.28±0.17	1.40±0.12	1.50±0.17
<i>P value</i>	<0.001						

Caudate nucleus head (Left)	0.98±0.15	1.18±0.14	1.27±0.18	1.23±0.14	1.29±0.18	1.43±0.11	1.52±0.17
<i>P value</i>	<0.001						
Thalamus (Right)	3.41±0.28	4.09±0.40	4.22±0.50	3.89±0.30	4.09±0.56	4.47±0.54	4.38±0.40
<i>P value</i>	<0.001						
Thalamus (Left)	3.47±0.30	4.14±0.41	4.24±0.48	3.92±0.35	4.13±0.54	4.44±0.50	4.33±0.39
<i>P value</i>	<0.001						
The largest brain area	127.91±14.09	149.70±5.54	154.86±11.57	159.20±6.91	156.57±13.38	161.50±10.42	169.94±9.72
<i>P value</i>	<0.001						
Corpus callosum area	3.72±0.75	4.33±0.41	4.79±0.60	3.46±0.22	4.39±0.47	5.39±0.99	6.17±0.92
<i>P value</i>	<0.001						

Table 6. Use of our methods concerning the features across different cases.

Case	Scaling				One-Hot-Encoding			Feature Selection
	Age	Gender	Age groups	Other Features	Gender	Age groups	Other Features	
A	✗	✗	✗	✗	✗	✗	✗	✗
B	✗	✗	✗	✓	✗	✗	✗	✗
C	✓	✗	✗	✓	✗	✗	✗	✗
D	✗	✗	✗	✗	✓	✓	✗	✗
E	✓	✗	✗	✓	✓	✓	✗	✗
F	✗	✗	✗	✗	✓	✓	✗	✓

✗ mark shows that the respective step is not applied, ✓ mark shows that the respective is applied

Age groups contain seven groups: 0-1 years (13 participants having epilepsy); 2-3 years (16 participants having epilepsy); 4-6 years (20 participants having epilepsy); 7 years (10 participants having epilepsy); 8- years (9 participants having epilepsy); 10-11 years (12 participants having epilepsy) and 12 years and over (21 participants having epilepsy).

Table 7. Obtained f1-scores of classifiers across different cases except for the F.

Case	ML Model (Classifier)									
	MLP	DT	NB	MNB	KNN	SVM	GBC	RF	AB	LR
A	0.490	0.656	0.520	0.417	0.484	0.407	0.710	0.689	0.675	0.521
B	0.387	0.651	0.520	0.413	0.554	0.393	0.698	0.672	0.681	0.524
C	0.385	0.652	0.520	0.427	0.557	0.389	0.709	0.665	0.681	0.543
D	0.426	0.663	0.521	0.431	0.507	0.407	0.734	0.623	0.652	0.527
E	0.605	0.651	0.512	0.432	0.564	0.560	0.724	0.640	0.653	0.494

Multi-Layer Perceptron (MLP); Decision Tree (DT); Naïve Bayes (NB); Multinomial NB (MNB); *k*-Nearest Neighbor (KNN); Support Vector Machine (SVM); Gradient Boosting Classifier (GBC); Random Forest (RF); Random Forest (RF); Logistic Regression (LR); AdaBoost (AB)

Table 8. The most informative four features and their goodness scores in the case of F across five folds.

Feature	Its goodness score at fold ...				
	1	2	3	4	5
Left amygdala	15.09074	✗	✗	8.746722	5.031380
Right amygdala	3.140098	0.118318	0.016722	0.828592	0.221019
Left insular cortex	0.308837	1.902834	1.925893	0.232817	0.791133
Right insular cortex	7.615912	3.450001	4.990626	8.840389	2.459970
Left hippocampus head	✗	7.216746	✗	✗	✗
Right hippocampus head	✗	✗	✗	✗	✗
Corpus collasum area	✗	✗	0.058654	✗	✗

The ✗ mark means that the respective feature is not selected at the respective fold.

DISCUSSION

Childhood is an important period of brain development, especially the first year of life, when important motor and cognitive milestones are achieved, it is an important period for brain development and maturation, microstructural changes occur and brain volume doubles^{6,7}. As brain development continues, synaptic connections initially form rapidly, which is reflected by an increase in grey matter volume. This is followed by an increase in white matter volume, which continues to increase until approximately 10 years of age^{6,9}. Eventually, due to unused connections, grey matter volumes remain constant or decrease from the age of 10 years^{32,33}. Epilepsy is a chronic neurological disorder affecting approximately 1% of all children. The type and frequency of seizures may vary from mild to severe and may have significant effects on the child's life in many areas including academic and social difficulties^{6,34-38}. Seizures in pediatric patients can occur at any age and have a devastating effect on cognitive development and quality of life⁴. Nuyts et al., in their 28 peer-reviewed case-control study to examine structural brain damage in genetic generalised epilepsy, emphasised that quantitative changes were found in frontal, thalamic, basal nuclei, corpus callosum, hippocampus, insula and general brain volumes, and abnormalities were detected in the thalamocortical network and neurocognitive functions. Additionally, there were grey matter volume abnormalities in the insula and gyrus frontalis medius in patients with epilepsy, and it was also emphasized that the reason for structural brain abnormalities in the grey matter volume in the insula and gyrus frontalis medius was related to the fact that they contributed to these deficits in attention networks¹⁰.

The complex structural and functional anatomy of the limbic system, including its connections and relationships with other brain regions, is reported to be essential for a better understanding of various disorders such as epilepsy, dementia, anxiety disorders, and schizophrenia. Wagner et al. have indicated that volumetric measurements of limbic system components in the pediatric age group can be valuable for comparative studies even when normative data are limited. Furthermore, these measurements may prove clinically useful by aiding treatment planning, disease monitoring, and providing reference data³⁹. Subcortical structures, including the hippocampus and thalamus, which are

frequently used in neuroimaging studies for epilepsy classification, play a crucial structural and functional role in the pathogenesis of epilepsy. In a study by Lucas and colleagues, MRI-based structural neuroimaging was performed on 42 patients with drug-resistant epilepsy and 13 healthy controls, revealing a significant volume reduction in hippocampal subfields as well as in several ipsilateral and contralateral thalamic nuclei⁴⁰.

The corpus callosum (CC) is the primary and largest commissural pathway connecting both cerebral hemispheres. The integration of the information process between both hemispheres takes place in this specialized area. The functional anatomy of the CC is also known to provide more useful and controlled information by integrating it into neurosurgical procedures in epilepsy surgery or intraventricular lesions^{5,41-44}. Due to the functional and anatomical characteristics of the corpus callosum, the corpus callosum is more sensitive and vulnerable to some pathologies. The corpus callosum could also contribute to rapid spread of seizure activities from one hemisphere to the other hemisphere, causing seizure generalization and epileptic spasm^{5,14,15,45}.

Sharifi et al. reported in an MRI study on corpus callosum (CC) morphometry in epilepsy patients that, although the CC is not a seizure onset site, it may serve as a primary pathway during seizures, indicating a link between epilepsy and the CC. The study also noted that about 50% of epilepsy patients show abnormal MRI findings, with hippocampal sclerosis being the most common. The temporal lobe was the most affected region (64.7%), followed by the frontal lobe (20%)⁴⁴. In an MRI study conducted by Pulsipher et al. investigating subcortical volume loss in epilepsy patients with temporal lobe involvement, volume reductions were observed, particularly in the hippocampus and corpus callosum, compared to healthy controls⁴⁶. In this study, the corpus callosum (CC) area was $4.87 \pm 1.15 \text{ cm}^2$ in healthy subjects and $4.49 \pm 1.14 \text{ cm}^2$ in epilepsy patients ($p=0.032$). While no significant gender differences were observed in healthy individuals, a significant difference was found in epilepsy patients ($p=0.030$). The CC area in epilepsy patients increased with age, ranging from 3.21 cm^2 (0–1 years) to 5.56 cm^2 (>12 years), with a significant difference between age groups ($p<0.001$). In a 2020 study conducted by Bennett et al. in the UK, the relationship between subcortical nuclei volume and cognitive function was examined in children with post-convulsive status epilepticus

(mean age 8.4 years). Compared to healthy controls, significantly reduced volumes were found in both the right ($p = 0.003$) and left ($p = 0.005$) caudate nuclei in children with cognitive impairments. Although children with epilepsy but without cognitive deficits showed lower volumes than healthy controls, these differences were not statistically significant (right, $p = 0.213$; left, $p = 0.359$). Thus, Bennett et al. demonstrated that cognitive decline associated with epilepsy is linked to volume reduction in subcortical structures⁴⁷. Sak NG conducted an MRI study on 118 children with epilepsy (0-5 years), 62 with febrile convulsions, and 50 healthy controls. Caudate nucleus volumes were higher in healthy male controls than in epilepsy patients aged 0-60 months, but the differences were not statistically significant on either side⁵. In our study, the caudate nucleus head area was lower on both the right and left sides in children with epilepsy compared to healthy children, although the difference was not statistically significant. Regarding gender, males had higher values than females in both groups.

Allusaini et al. found that healthy controls had significantly larger bilateral hippocampal volumes compared to 75 temporal lobe epilepsy patients with hippocampal sclerosis. The epilepsy group showed significant volume loss in the ipsilateral amygdala, while bilateral amygdala reduction in patients with bilateral hippocampal sclerosis was not significant. The study also suggested that longer disease duration may contribute to volume loss in these brain regions⁴⁸. To investigate the macro- and microstructural changes that epilepsy may cause in central nervous system (CNS) regions, MacEachern et al. conducted an MRI study on 30 children with epilepsy and healthy controls, finding significant volume reductions in the putamen ($p=0.037$), amygdaloid complex ($p=0.045$), and thalamus ($p<0.001$) in the epilepsy group. They also reported microstructural changes in highly connected regions like the thalamus and putamen, suggesting these areas are especially vulnerable to seizure activity⁶. These findings emphasize the critical role of subcortical structures in epilepsy pathology and suggest that targeted treatments for these vulnerable brain regions may improve clinical outcomes. The thalamus, closely connected to the basal nuclei, serves as a central communication hub for normal and abnormal electrical impulses and plays a critical role in epilepsy pathophysiology and seizure control through its extensive cortical connections. While it is commonly implicated in seizure propagation and secondary

generalization, some studies report that the thalamus may not be involved in certain epilepsy types. Its diverse functions within cortical networks and widespread CNS connections make it especially vulnerable to activation-induced microstructural changes, which are thought to precede macrostructural alterations during disease progression^{2,5}. Unlike other studies, Legouhy et al. conducted a study in the UK with 53 healthy controls and 143 epilepsy patients, evaluating the volume of the amygdaloid complex and reporting larger volumes in epilepsy patients. Additionally, they found reduced neurite density in regions regulating cardiovascular and respiratory functions, noting that this disruption negatively affects blood pressure and respiratory control, thereby increasing the risk of sudden death. It was also stated that the volume increase likely reflects structural disorganization rather than improved function, with excitotoxic damage and inflammatory processes possibly contributing to this change⁴⁹.

The hippocampus plays a crucial role not only in memory and cognitive functions but also in the initiation and propagation of seizures, making its function significantly impaired in epilepsy and cognitive decline. Moreover, Lucas et al. (2024) noted structural and functional changes in the hippocampus and thalamus in epilepsy⁴⁰. Hermann et al. (2007) reported increased frontal gray matter and decreased brainstem volume in children with both epilepsy and ADHD⁵⁰. Cardamone et al. identified the hippocampus and amygdala as key regions in epilepsy and depression, involved in regulating stress responses through feedback loops. They also emphasized hippocampal neuroplasticity, its link to neurological disorders, and its role as a common seizure initiation site, with impaired neuroplasticity being typical in acquired epilepsy⁵¹. Machine learning (ML) is widely used due to its proven success across various fields. In this study, a basic ML pipeline was developed using different methods. The results showed that scaling the dataset features did not improve the F1 score, as it reduced the discriminative power of certain features by giving equal weight to all. In our case, some features are more informative due to their natural value ranges. Conversely, one-hot encoding applied to only gender and age was beneficial, as it prevented these features from gaining disproportionate importance. Encoding categorical variables as integers can mislead the model into assigning more weight to them, whereas one-hot encoding distributes this weight more evenly. Feature

selection also contributed positively by identifying the most relevant features. The best F1 score achieved was 0.771, indicating that the model can correctly classify 77 out of 100 children as either having or not having epilepsy. Given that machine learning models tend to generalize more effectively with larger datasets, the proposed model may assist healthcare professionals in their decision-making process, and its performance can be further enhanced through training on expanded data collections.

This study's sample size, while adequate, remains relatively small and may limit the generalizability of the findings across the diverse pediatric epilepsy population. Additionally, the cross-sectional design restricts our ability to assess longitudinal changes in brain structure and seizure progression. Future research should incorporate larger, multicenter cohorts with longitudinal follow-up to better understand the dynamic neurodevelopmental changes in pediatric epilepsy. Moreover, integrating multimodal imaging and clinical data could enhance the accuracy of machine learning models and provide deeper insights into the heterogeneity of epilepsy phenotypes in children. Emphasizing early detection and personalized treatment strategies in future studies will be critical to improving outcomes in this vulnerable population.

In conclusion, this study compared brain region volumes between pediatric epilepsy patients and healthy controls, alongside an innovative machine learning (ML) evaluation. By developing a robust ML pipeline incorporating various techniques, we showed that automatic epilepsy detection in children achieves high accuracy, especially with feature selection. Model performance can improve further with larger datasets. Additionally, understanding neural disruptions in epilepsy such as altered reward processing, learning deficits, and impaired connectivity involving the basal nuclei, thalamus, and corpus callosum can enhance quality of life, seizure control, and personalized treatment. This study highlights epilepsy's widespread impact on multiple brain regions and the influence of age and gender on these changes, paving the way for more precise diagnostics and therapies in pediatric epilepsy.

Author Contributions: Concept/Design : KK, MÖ, BD, ÖK, ÖÇ, NB, PG, SP; Data acquisition: KK, MÖ, Fİ, BD, ÖK, SP; Data analysis and interpretation: MÖ, Fİ, KK, ÖÇ, SP; Drafting manuscript: KK, ÖÇ, SP; Critical revision of manuscript: Fİ, ÖÇ, MÖ, NB, MT, PG, SP; Final approval and accountability: KK, MÖ, Fİ, BD, ÖK, ÖÇ, NB, MT, PG, SP; Technical or material support: KK, MÖ, BD, ÖK, Fİ, SP; Supervision: SP, ÖÇ, Fİ, MÖ; Securing funding (if available): n/a.

Ethical Approval: Ethical approval was obtained from the Çukurova University Faculty of Medicine Non-Interventional Clinical Research Ethics Committee with the decision number 136/43 dated 01.09.2023.

Peer-review: Externally peer-reviewed.

Conflict of Interest: Authors declared no conflict of interest.

Financial Disclosure: Authors declared no financial support

This study was supported by Çukurova University Scientific Research Projects with the project number TYL- 2023-16343.

REFERENCES

1. Canpolat M. Canpolat Temel Pediatrik Epilepsi. Ankara, Akademisyen Kitabevi, 2014.
2. Whelan CD, Altmann A, Botiá JA, Jahanshad N, Hibar DP, Absil J et al. Structural brain abnormalities in the common epilepsies assessed in a worldwide ENIGMA study. *Brain*. 2018;141:391-17.
3. Woźniak MM, Zbroja M, Matuszek M, Pustelniak O, Cyranka W, Drelich K et al. Epilepsy in pediatric patients-evaluation of brain structures' volume using VolBrain software. *J Clin Med*. 2022;11:4657.
4. Frank NA, Greuter L, Guzman R, Soleman J. Early surgical approaches in pediatric epilepsy - a systematic review and meta-analysis. *Childs Nerv Syst*. 2023;39:677-11.
5. Sak NG. Epilepsi tanısı konmuş çocuklarda bazı beyin yapılarındaki hacimsel ve morfolojik değişikliklerin manyetik rezonans görüntüleme yöntemi ile incelenmesi ve febril konvulsiyonla ilişkisi: Retrospektif bir çalışma. Doctoral thesis, Bursa Uludağ University, Bursa, 2023.
6. MacEachern SJ, Santoro JD, Hahn KJ, Medress ZA, Stecher X, Li MD et al. Children with epilepsy demonstrate macro and microstructural changes in the thalamus, putamen, and amygdala. *Neuroradiology*. 2020;62:389-8.
7. Gilmore JH, Lin W, Prastawa MW, Looney CB, Vetsa YS, Knickmeyer RC et al. Regional gray matter growth, sexual dimorphism, and cerebral asymmetry in the neonatal brain. *J Neurosci*. 2007;27:1255-5.
8. Knickmeyer RC, Gouttard S, Kang C, Evans D, Wilber K, Smith JK et al. A structural MRI study of human brain development from birth to 2 years. *J Neurosci*. 2008;28:12176-6.
9. Sampaio RC, Truwit CL. Myelination in the developing human brain. *Handbook of developmental cognitive neuroscience*. Cambridge, MIT. 2001.
10. Nuyts S, D'Souza W, Bowden SC, Vogrin SJ. Structural brain abnormalities in genetic generalized epilepsies: A systematic review and meta-analysis. *Epilepsia*. 2017;58:2025-12.
11. Rejdak K, Rola R, Mazurkiewicz-Beldzińska M, Halczuk I, Błaszczyk B, Rysz A et al. Diagnosis and treatment of epilepsy in adults—Recommendations of the Polish Neurological Society. *Pol Przegląd Neurol*. 2016;12:15–12.

12. Siemianowski C, Królicki L. Importance of neuroimaging methods in the diagnosis of epilepsies. *Pol Przegląd Neurol.* 2005;1:76–4.
13. Spencer D. MRI (minimum recommended imaging) in epilepsy. *Epilepsy Curr.* 2014;14:261-2.
14. Ghani Zghair MA. Corpus callosum disorders and associated malformations in paediatric epilepsy: MRI analytic study. *J Pak Med Assoc.* 2021;71:S190.
15. Okanishi T, Fujimoto A. Corpus callosotomy for controlling epileptic spasms: A proposal for surgical selection. *Brain Sci.* 2021;11:1601.
16. Rao S, Poojary P, Somaiya J, Mahajan P. A comparative study between various preprocessing techniques for machine learning. *Int J Eng Appl Sci Technol.* 2020;5:2455-12.
17. Dahouda MK, Joe I. A deep-learned embedding technique for categorical features encoding. *IEEE Access.* 2021;9:114381-10.
18. Coban O. A new modification and application of item response theory-based feature selection for different machine learning tasks. *Concurrency Computat Pract Exper.* 2022;34:e7282.
19. Johnson KJ, Synovec RE. Pattern recognition of jet fuels: comprehensive GC×GC with ANOVA-based feature selection and principal component analysis. *Chemometr Intell Lab Syst.* 2002;60:225-12.
20. Coban O. An assessment of nature-inspired algorithms for text feature selection. *Computer Science.* 2022;23:179-25.
21. Popescu MC, Balas VE, Perescu-Popescu L, Mastorakis N. Multilayer perceptron and neural networks. *WSEAS Trans Circuits Syst.* 2009;8:579-9.
22. Dhall D, Kaur R, Juneja M. Machine learning: a review of the algorithms and its applications. *Proceedings of ICRIC 2019: Recent innovations in computing.* 2020;47-16.
23. Dash SS, Nayak SK, Mishra D. A review on machine learning algorithms. *Intelligent and Cloud Computing: Proceedings of ICICC 2019.* 2020;2:495-12.
24. Su J, Shirab JS, Matwin S. Large scale text classification using semi-supervised multinomial naive bayes. *ICML.* 2011;97-7.
25. Coban O, Sehitoglu E, Yaganoglu M. Predicting child development status: Can machine learning Help?. In *2024 4th International Conference on Emerging Smart Technologies and Applications (eSmarTA).* 2024;1-6.
26. Sahin EK. Comparative analysis of gradient boosting algorithms for landslide susceptibility mapping. *Geocarto Int.* 2022;37:2441-24.
27. Kleinbaum DG, Dietz K, Gail M, Klein M, Klein M. *Logistic regression.* New York, Springer-Verlag, 2002.
28. Pedregosa F, Varoquaux G, Gramfort A, Michel V, Thirion B, Grisel O et al. Scikit-learn: Machine learning in Python. *J Mach Learn Res.* 2011;12:2825-30.
29. Kohavi R. *A study of cross-validation and bootstrap for accuracy estimation and model selection.* Morgan Kaufman Publishing, 1995.
30. McKinney W. pandas: a foundational Python library for data analysis and statistics. *Python for high performance and scientific computing.* 2011;14:1-9.
31. Harris CR, Millman KJ, van der Walt SJ, Gommers R, Virtanen P, Cournapeau D et al. Array programming with NumPy. *Nature.* 2020;585:357-5.
32. Magiorkinis E, Sidiropoulou K, Diamantis A. Hallmarks in the history of epilepsy in antiquity. *Epilepsy Behav.* 2010;17:103-5.
33. Forkert ND, Li MD, Lober RM, Yeom KW. Gray matter growth is accompanied by increasing blood flow and decreasing apparent diffusion coefficient during childhood. *Am J Neuroradiol.* 2016;37:1738-6.
34. Katyayan A, Diaz-Medina G. Epilepsy: Epileptic syndromes and treatment. *Neurol Clin.* 2021;39:779-16.
35. Guerrini R. Epilepsy in children. *Lancet.* 2006;367:499-5.
36. Hauser WA, Annegers JF, Kurland LT. Incidence of epilepsy and unprovoked seizures in Rochester, Minnesota: 1935-1984. *Epilepsia.* 1993;34:453-15.
37. MacEachern SJ, D'Alfonso S, McDonald RJ, Thornton N, Forkert ND, Buchhalter JR. Most children with epilepsy experience postictal phenomena, often preventing a return to normal activities of childhood. *Pediatr Neurol.* 2017;72:42-50.e3.
38. Danguedan AN, Smith ML. Academic outcomes in individuals with childhood-onset epilepsy: mediating effects of working memory. *J Int Neuropsychol Soc.* 2017;23:594-10.
39. Wagner MW, Rafful PP, Vidarsson L, Ertl-Wagner BB. MRI volumetric analysis of the hypothalamus and limbic system across the pediatric age span. *Children (Basel).* 2023;10:477.
40. Lucas A, Mouchtaris S, Tranquille A, Sinha N, Gallagher R, Mojena M et al. Mapping hippocampal and thalamic atrophy in epilepsy: A 7-T magnetic resonance imaging study. *Epilepsia.* 2024;65:1092-14.
41. Yıldırım M. *Temel Nöroanatomi.* İstanbul, Nobel Tıp, 2014.
42. Dere F. *Atlaslı Nöroanatomi Fonksiyonel Nöroloji.* Ankara, Nobel Tıp i, 2012.
43. Taner D. *Fonksiyonel Nöroanatomi.* Ankara, ODTÜ Yayıncılık, 2011.
44. Sharifi Y, Rahimian E, Razaati A, Tafakhori A. Measurements of the corpus callosum in epileptic patients Using Magnetic Resonance Imaging. *Research Square.* 2023.
45. Chen PC, Messina SA, Castillo E, Baumgartner J, Seo JH, Skinner H et al. Altered integrity of corpus callosum in generalized epilepsy in relation to seizure lateralization after corpus callosotomy. *Neurosurg Focus.* 2020;48:E15.

46. Pulsipher DT, Seidenberg M, Morton JJ, Geary E, Parrish J, Hermann B. MRI volume loss of subcortical structures in unilateral temporal lobe epilepsy. *Epilepsy Behav.* 2007;11:442-9.
47. Bennett KH, Pujar SS, Martinos MM, Clark CA, Yoong M, Scott RC et al. Subcortical nuclei volumes are associated with cognition in children post-convulsive status epilepticus: Results at nine years follow-up. *Epilepsy Behav.* 2020;110:107119.
48. Alhusaini S, Doherty CP, Scanlon C, Ronan L, Maguire S, Borgulya G et al. A cross-sectional MRI study of brain regional atrophy and clinical characteristics of temporal lobe epilepsy with hippocampal sclerosis. *Epilepsy Res.* 2012;99:156-10.
49. Legouhy A, Allen LA, Vos SB, Oliveira JFA, Kassinosopoulos M, Winston GP et al. Volumetric and microstructural abnormalities of the amygdala in focal epilepsy with varied levels of SUDEP risk. *Epilepsy Res.* 2023;192:107139.
50. Hermann B, Jones J, Dabbs K, Allen CA, Sheth R, Fine J et al. The frequency, complications and aetiology of ADHD in new onset paediatric epilepsy. *Brain.* 2007;130:3135-13.
51. Cardamone L, Salzberg MR, O'Brien TJ, Jones NC. Antidepressant therapy in epilepsy: can treating the comorbidities affect the underlying disorder?. *Br J Pharmacol.* 2013;168:1531-23.